Supporting Information

Single-wavelength phototheranostics for colon cancer *via* thiolytic reaction

Yucheng Zhu,‡[a] Chao Chen,‡[b] Qinghua Wu,[c] Guoliang Yang,[a] Zhiyong Liu,[a] Erhong Hao,[c] Hongliang Cao,[a] Yun Gao[a] and Weian Zhang*[a]

[a]Shanghai Key Laboratory of Functional Materials Chemistry, School of Materials Science and Engineering, East China University of Science and Technology, 130 Meilong Road, Shanghai 200237, China.
[b]State Key Laboratory of Bioreactor Engineering Center, School of Biotechnology, East China University of Science and Technology, 130 Meilong Road, Shanghai 200237, China.
[c]Laboratory of Functional Molecular Solids, Ministry of Education, Anhui Laboratory of Molecule Based Materials (State Key Laboratory Cultivation Base) and School of Chemistry and Materials Science, Anhui Normal University. No. 1 East Beijing Road, Wuhu, 241000, Anhui, China.

Materials

All the reactions were performed under an atmosphere of nitrogen and all the chemicals were obtained from Shanghai Titan Scientific Co.,Ltd. unless otherwise noted. Triethylene glycol monomethyl ether, 2,4-dimethylpyrrole, 4-hydroxybenzaldehyde, 2,3-dichloro-5,6-dicyano-*p*-benzoquinone, $BF_3{\cdot}OEt_2$, 2,4-dinitro-fluorobenzene and 1,3-diphenylisobenzofuran (DPBF) were purchased from Shanghai Titan Scientific Co.,Ltd. tetrahydrofuran (THF) and toluene were dried by refluxing over sodium shavings and distilled just prior to use. *N*, *N*-dimethylformamide (DMF), triethylamine (TEA) and dichloromethane (CH_2Cl_2) were dried over CaH_2 and distilled just prior to use. 4′,6-diamidino-2-phenylindole (DAPI) and thiazolyl blue tetrazolium bromide (MTT) were purchased from Aladdin and used as received. 2′,7′-dichlorofluorescin diacetate (DCFH-DA, ROS probe) was obtained from the Beyotime Institute of Biotechnology (Shanghai, China).

Characterization

BRUKER AV400 spectrophotometer was used to measure the ^1H NMR of the samples which were dissolved in $CDCl_3$ with tetramethylsilane (TMS) as an internal reference. Transmission electron microscopy (TEM) was performed on a JEOL JEM1400 electron microscope operated at 100 kV. The sample for TEM was prepared by directly dropping the self-assembled aqueous solution (0.2 mg mL^{-1}) onto a carbon-coated copper grid, and the sample was measured until the solution dried at ambient temperature. Fluorescence spectra (FS) was recorded with an F-4500 fluorescence spectrometer and absorption spectrum was performed by a Shimadzu UV-2550 UV-Visible spectrophotometer using a quartz cuvette with 1 cm beam path length. Hydrodynamic diameter (D_h) was measured by dynamic light scattering (DLS) using a BECKMAN COULTER Delasa Nano C particle analyzer with the wavelength of 532 nm at 25 °C and the scattering angle was 165 °.

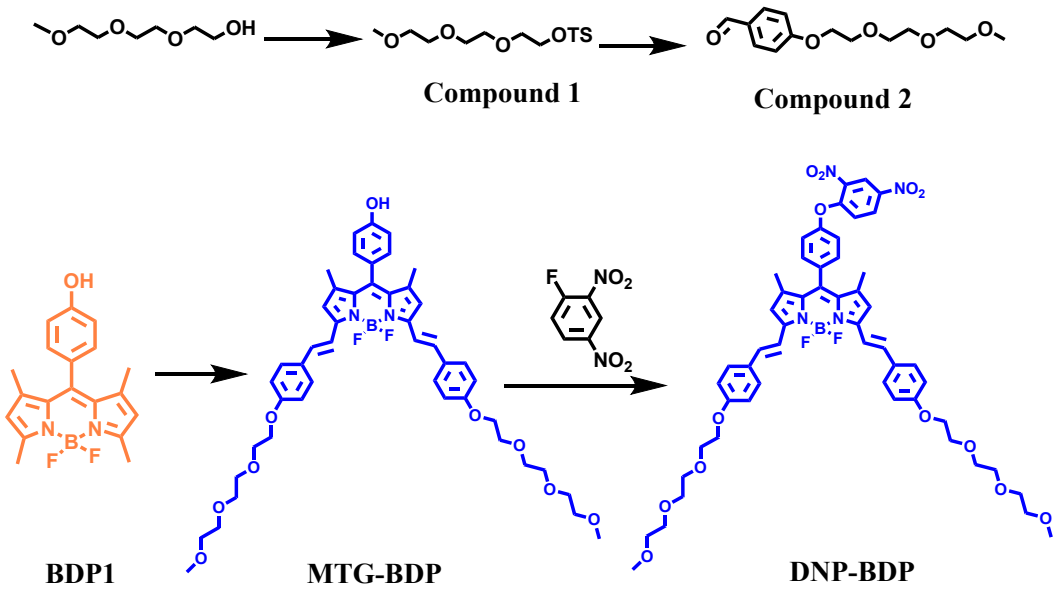

Scheme S1. Schematic illustration for the synthesis of DNP-BDP.

Synthesis of Compound 1

Compound 1 was synthesized according to reported procedures. [1] The final product was characterized by ^{1}H NMR as shown in **Fig. S1**.

Synthesis of Compound 2

4-hydroxybenzaldehyde (1.23 g, 10 mmol) and compound **1** (4.8 g, 15 mmol) were dissolved in 50 ml acetonitrile. K_2CO_3 (3.2 g, 22.4 mmol) and a few crystals of benzo-18-crown-6 were added. The reaction was refluxed until all 4-hydroxybenzaldehyde was consumed. The solvent was evaporated in vacuo, extracted with water and CH_2Cl_2. Organic layer was dried with Na_2SO_4 and evaporated under reduced pressure. The product was purified by silica gel column chromatography using CH_2Cl_2/Hexane (4:1, v/v). Fraction containing compound **2** was collected then the solvent was removed under reduced pressure (2.1 g, 78%). The final product was characterized by ^{1}H NMR in **Fig. S2**. ^{1}H NMR ($CDCl_3$, 400 MHz): 9.80 (s, 1H), 7.75 (d, J = 7.42 Hz, 2H), 6.94 (d, J = 7.81 Hz, 2H), 4.13 (m, 2H), 3.80 (m, 2H), 3.70-3.40 (m, 8H), 3.27 (s, 3H).

Synthesis of BDP 1

To a solution of 4-hydroxybenzaldehyde (0.318 g, 2.6 mmol) and 2,4-dimethylpyrrole (0.5 g, 5.26 mmol) in THF (50 mL) was added several drops of trifluoroacetic acid. The mixture was stirred at ambient temperature overnight, then a solution of 2,3-dichloro-5,6-dicyano-*p*-benzoquinone (0.509 g, 2.6 mmol) in THF (50 mL) was added. The mixture was stirred continuously for another 2 h. After the addition of triethylamine (10 mL), $BF_3{\cdot}OEt_2$ (10 mL) was added dropwise to the mixture, which was cooled in an ice-water bath. The mixture was kept stirring at ambient temperature overnight, then filtered through a celite pad. The residue was washed with CH_2Cl_2 (50 mL), then the combined filtrate was rotary evaporated to dryness. The residue was redissolved in CH_2Cl_2 (100 mL) and the solution was washed with 5% aqueous $NaHCO_3$ solution (100 mL) followed with water (100 mL × 2). The organic portion was dried over anhydrous $MgSO_4$, then evaporated in vacuo. The crude product was purified by silica gel column chromatography using CH_2Cl_2 as the eluent to give BDP1 as a red solid (0.4 g, 49%). The final product was characterized by ^{1}H NMR in **Fig. S3**.

Synthesis of MTG-BDP

BDP1 (0.340 g, 1 mmol) and compound 2 (1.073 g, 4 mmol) were added to a 500 mL round-bottomed flask containing 200 mL benzene and to this solution was added piperidine (1.2 mL) and acetic acid (1 mL). Then the mixture was refluxed overnight using Dean-Stark apparatus under the nitrogen atmosphere. When all the starting material had been consumed, the mixture was cooled to room temperature and solvent was evaporated. Water (100 mL) added to the residue and the product was extracted into the chloroform (100 mL × 3). Organic phase dried over anhydrous $MgSO_4$ and then concentrated under reduced pressure. The crude product was purified by silica gel column chromatography using ethyl acetate/hexane (1:1, v/v) to give MTG-BDP as a blue solid (0.05 g, 20%). The final product was characterized by ^{1}H NMR in **Fig. S4** and ^{13}C NMR in **Fig. S5**. ^{1}H NMR (400 MHz, DMSO): δ 9.88 (s, 1H), 7.57 (d, *J* = 8.8 Hz, 4H), 7.50 (s, 2H), 7.39 (d, *J* = 16.3 Hz, 2H), 7.18 (d, *J* = 8.5 Hz, 2H), 7.05 (d, *J* =

8.8 Hz, 2H), 6.94 (d, *J* = 8.8 Hz, 2H), 4.24-4.10 (m, 4H), 3.89-3.72 (m, 4H), 3.52 (m, 16H), 3.24 (s, 4H), 1.50 (s, 4H). MALDI-TOF: m/z 840.3606 [M], 821.3643 $[M-F]^+$ (**Fig. S6**).

Synthesis of DNP-BDP

MTG-BDP (0.073 g, 0.085 mmol) and 2,4-dinitro-fluorobenzene (0.063 g, 0.34 mmol) were dissolved in anhydrous DCM (50 mL) under the protection of N_2 atmosphere. Then, two or three drops of triethylamine were added at 0 ℃. After 30 min, the reaction mixture was stirred overnight at room temperature. The concentrated mixture was dissolved in DCM and then washed with water, brine and dried with Na_2SO_4. Then the residue was purified by a flash column chromatography and the blue solid product was obtained. Yield: 0.25 g (49.4%). The final product was characterized by ^{1}H NMR (**Fig. S7**) and ^{13}C NMR in **Fig S8**. ^{1}H NMR (400 MHz, DMSO): 8.93 (d, *J* = 2.8 Hz, 1H), 8.58 (d, *J* = 9.2, 2.8 Hz, 1H), 7.58 (m, *J* = 19.9, 9.8 Hz, 6H), 7.43 (m, *J* = 19.7, 12.5 Hz, 4H), 7.24 (d, *J* = 9.2 Hz, 1H), 7.06 (d, *J* = 8.8 Hz, 6H), 6.99 (s, 2H), 4.21-4.09 (m, 4H), 3.83-3.72 (m, 4H), 3.66-3.40 (m, 16H), 3.24 (s, 6H), 1.52 (s, 6H). MALDI-TOF: m/z 987.4033 $[M-F]^+$ (**Fig. S9**).

Self-assembly of FR-H_2S

As a typical nanoprecipitation method, DNP-BDP (0.5 mg) was first dissolved in 1 mL DMF to form the solution with a concentration of 0.5 mg mL^{-1}. Then 1 mL of above solution was added dropwise into 4 mL of distilled water under magnetic stirring at ambient temperature for 0.5 h. The mixture solution was stirred for 3 h and dialyzed against distilled water using a dialysis membrane (MWCO = 1000) for 3 days.

Photostability

To evaluate the photostability of FR-H_2S. FR-H_2S buffer was irradiated using 650 nm laser (0.5 W cm^{-2}) for 5, 15, 30 and 60 min, respectively. Then, the UV/vis absorption

spectra of FR-H_2S was measured for the photostability.

Singlet Oxygen Detection

The singlet oxygen ($^1O_2$) generation yield of FR-H_2S was evaluated by singlet oxygen capture agent, 1, 3-diphenlisobenzofuran (DPBF). Briefly, the absorbance of DPBF at 415 nm was adjusted to about 1.0 in PBS, and FR-H_2S pretreated with NaHS was added to cuvette. The cuvette was then exposed to a 650 nm monochromatic laser for different time, and the corresponding absorption spectra was measured immediately. The slopes of absorbance of DPBF at 415 nm versus irradiation time were measured and used to compare the $^1O_2$ generation ability.

Photothermal Effect

To demonstrate the photothermal conversion behavior of FR-H_2S in the present of H_2S, the FR-H_2S solutions pretreated with H_2S were irradiated for 300 s in 0.2 mL glass vials at 650 nm laser irradiation and the temperature of solutions was measured by using an IR thermal camera at an interval of 30 s. The solutions of the NaHS pretreated FR-H_2S at the concentration of 0, 50, 100 and 200 μM in 0.2 mL vials were irradiated using 650 nm laser for 300s (1 W cm^{-2}). Moreover, the NaHS pretreated FR-H_2S at the concentration of 200 μM were irradiated by using a 650 nm laser at 0.6, 0.8 and 1 W cm^{-2} for 300 s. The photothermal stability FR-H_2S was confirmed when FR-H_2S solution (50 μM) was irradiated with a laser at 0.8 W cm^{-2} for 4 cycles. To verify the low temperature change of FR-H_2S without H_2S under laser irradiation, FR-H_2S at the concentration of 100 and 200 μM were irradiated by using a 650 nm laser at 0.5 W/cm^2.

Cell Cultures

HepG-2, MCF-7 and HCT116 cells were cultured in Dulbecco's modified Eagle's medium (DMEM) comprised of antibiotics (50 units mL^{-1} penicillin and 50 units mL^{-1} streptomycin) and 10% fetal bovine serum (FBS) at 37 °C in a humidified atmosphere

with 5% CO_2.

Cellular Uptake Studies

The cellular uptake experiments were carried out by confocal laser scanning microscope (CLSM). For CLSM measurement, HepG-2, MCF-7 and HCT116 cells were cultured in 2 mL culture medium on polylysine-coated glass slides inside 30 mm glass culture dishes and allowed to grow to 50-70% at 37 °C. Afterward, cells (on glass slides) were washed with PBS, and reincubated in DMEM medium containing the samples at 37 °C under 5% CO_2 for 24 h. After predetermined time, the culture medium was removed and washed with PBS three times. Subsequently, the 4, 6-diamidino-2-phenylindole (DAPI) was added to stain the nuclei for 15 min. The cells were imaged directly *via* CLSM after washing with PBS three times.

Intracellular ROS Detection

An ROS sensor dye, 2',7'-dichlorodihydrofluorescin diacetate acid (DCF-DA), was used to sense intracellular ROS upon 650 nm laser irradiation. HCT116 cells were cultured in fresh culture medium for 24 h and FR-H_2S were then incubated for 2 h in the dark, and then DCF-DA was added, after 20 min incubation, cells were washed three times with PBS and then exposed to 650 nm laser irradiation. After laser irradiation, cells were imaged by confocal laser scanning microscope.

In Vitro Dark Cytotoxicity and Phototoxicity

For in vitro phototoxicity, HCT116 cells (25000 cells mL^{-1}, 200 μL) were seeded into a 96-well plate and cultured for 24 h at 37 °C. The culture medium was replaced with a fresh culture medium containing FR-H_2S (DNP-BDP concentration at 0-80 μg mL^{-1}, respectively). After the cells were incubated for 24 h at 37 °C, they were irradiated using a laser (0.5 W cm^{-2}) for 10 min and then incubated for another 24 h. Thereafter, the culture medium was replaced with a fresh culture medium and 20 μL MTT (5 mg

mL^{-1}) for a further incubation of 4 h. Finally, the culture medium containing MTT was replaced with 150 μL DMSO to dissolve the precipitates, followed by measuring the absorbance of solution at 492 nm by THERMO Multiskan MK3 spectrometer, a spectrophotometric microplate reader. Cell viability was calculated by the Eqn (1):

$$\text{Cell viability (\%)} = (OD_t - OD_b) / (OD_c - OD_b) \times 100 \quad (1)$$

where OD_b is the absorbance of the background; OD_t and OD_c are the absorbance of solutions with or without samples, respectively. For in vitro dark cytotoxicity, the process was similar to the phototoxicity described above, but without the irradiation.

Animals and Tumor Models

Female BALB/c nude mice (4 to 6-week-old) were maintained in a pathogen free environment under controlled temperature (24 °C). The female nude mice were injected subcutaneously in the right leg region with 100 μL of cell suspension containing 5×10^6 HCT116 cells. The tumors were allowed to grow to ~100 mm^3 before experimentation. The tumor volume was calculated as (tumor length) × (tumor width)^2/2.

In Vivo Fluorescence Imaging

When the tumor volume reached 100 mm^3, FR-H_2S (200 μL, 2.5 mg / kg) were injected into the tail vein of nude mice. Fluorescence imaging was performed at 0.5, 4, 8 and 24 h after injection using an in vivo imaging system. And to confirm the H_2S selectiveness of FR-H_2S, fluorescent images were taken at various time points after subcutaneous injection of FR-H_2S into tumor and normal regions. Moreover, mice were euthanized and their tumors and major organs (heart, liver, spleen, kidneys and lungs) were imaged by a fluorescence imaging system.

In Vivo Photothermal Imaging

When the tumors grew to 100 mm^3, the five mice were intratumorally injected with the solution of FR-H_2S and PBS. The whole-body photothermal images of mice were taken 5 min after injection, respectively. The temperature variation of the tumor site was recorded by an IR thermal camera.

In Vivo Phototherapy

When the tumor volume reached about 100 mm^3, tumor-bearing mice were divided into seven groups (*n* = 4 mice/group) randomly for different formulations: (1) saline alone (Saline); (2) laser only (L); (3) FR-H_2S only (FR-H_2S) and (4) FR-H_2S plus light (FR-H_2S + L). The solution of different groups (200 μL, 1 mg mL^{-1}) was intravenously injected into mice and irradiated by the 650 nm laser (1 W cm^{-2}) for 15 min after 24 h and then the same irradiated performances were carried out during the following treament period. The tumor dimensions (length and width) and body weight were measured every two days during the treatment. The mice were sacrificed after 2 weeks post-treatment, the tumors were collected and photos were taken.

Tissue Immunohistological Evaluation

In the histological assay, the heart, liver, spleen, lung, kidney and tumor tissues were fixed in 4% paraformaldehyde for 24 h. The specimens were dehydrated in graded ethanol, embedded in paraffin, and cut into 5 mm thick sections. The fixed sections were deparaffinized and hydrated according to a standard protocol and stained with hematoxylin and eosin (H&E) for microscopic observation. Apoptosis of the tumor cells in the mice after treatments was determined by the TUNEL method according to the manufacturer's instructions.

Statistical Analysis

The data of the experiments were presented as mean ± standard deviation (SD). The one-way ANOVA analysis was used to determine the statistical significance using no significance: n.s, *P < 0.05, **P < 0.01, ***P < 0.001.

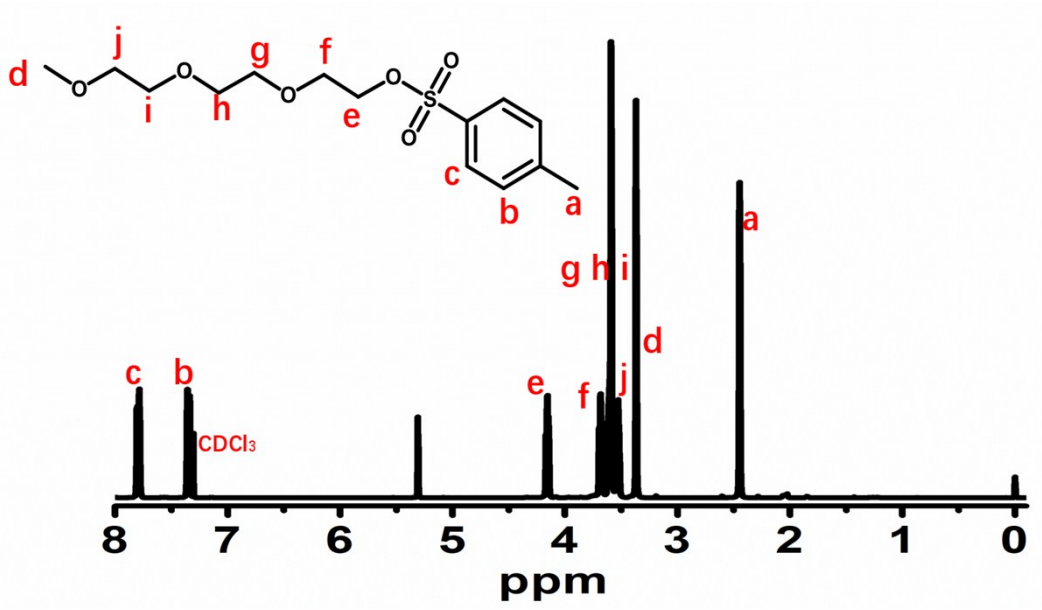

Figure S1. ^{1}H NMR spectrum of Compound 1.

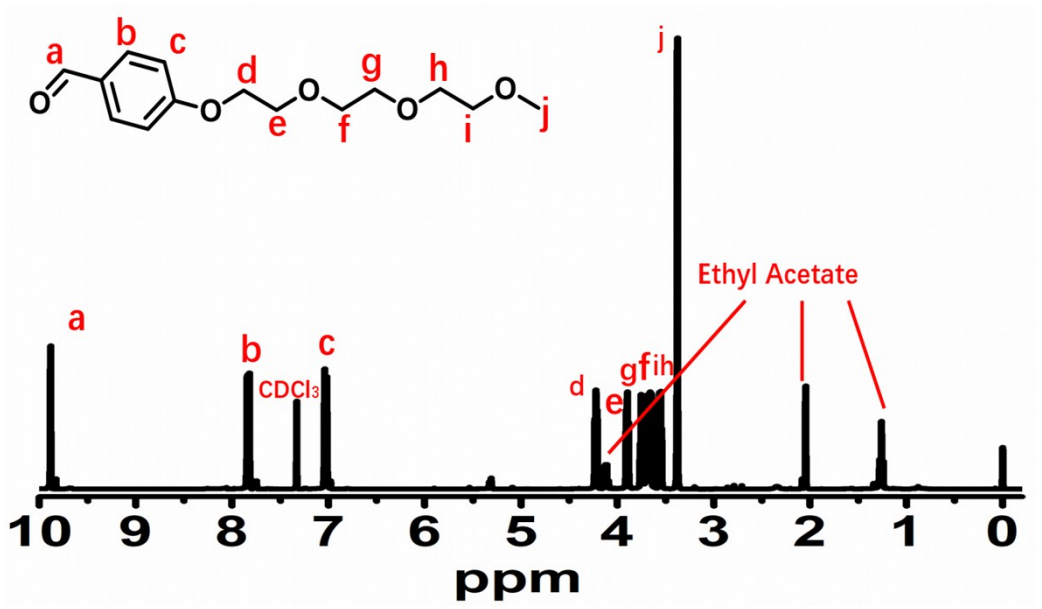

Figure S2. ^{1}H NMR spectrum of Compound 2.

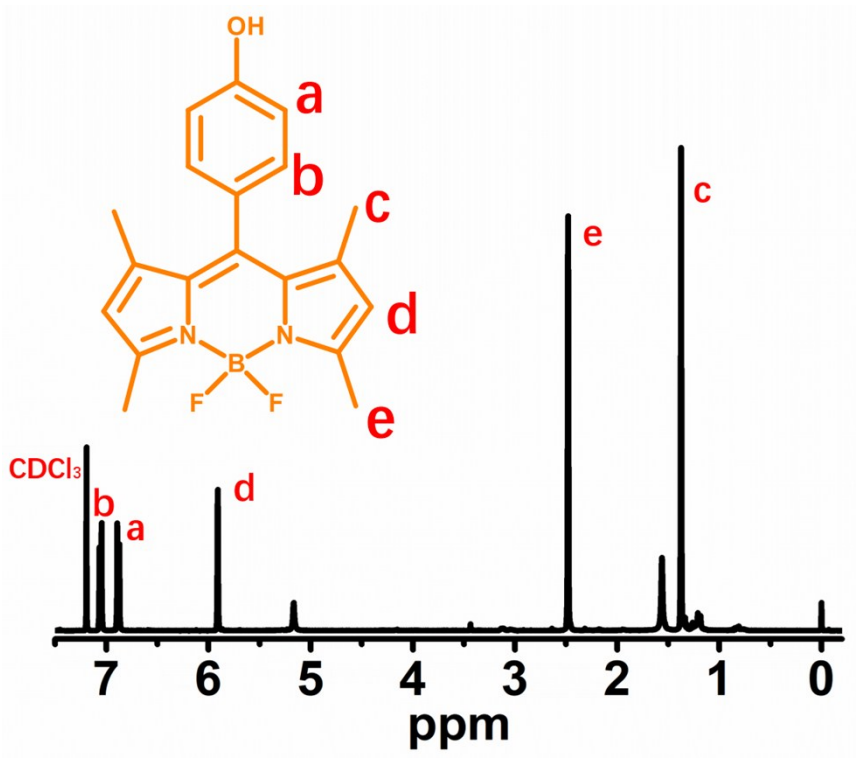

Figure S3. ^{1}H NMR spectrum of BDP1.

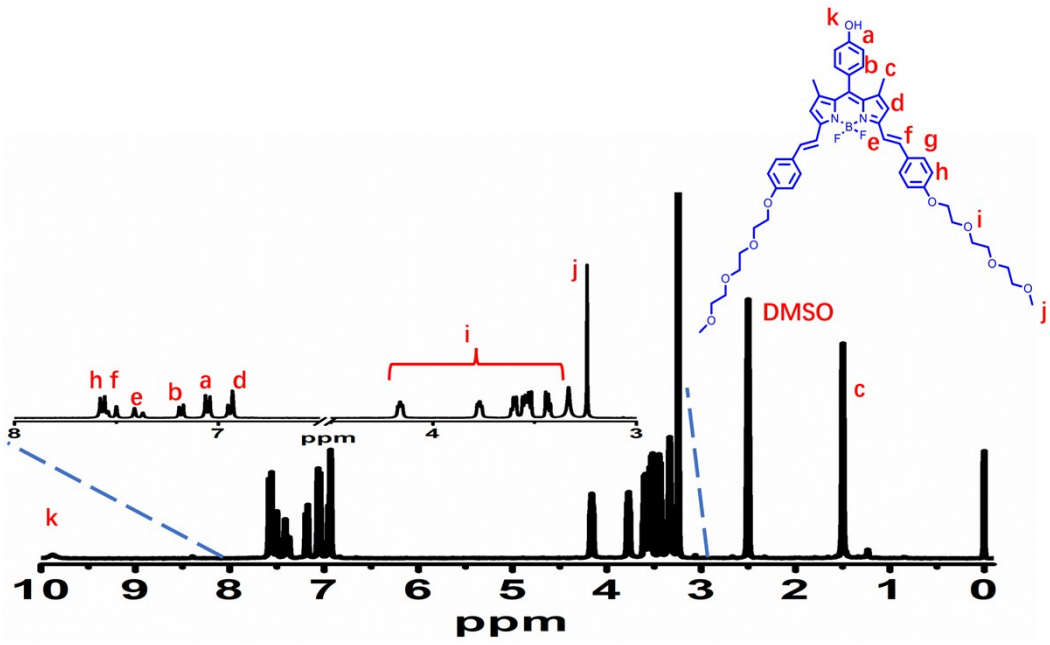

Figure S4. ^{1}H NMR spectrum of MTG-BDP.

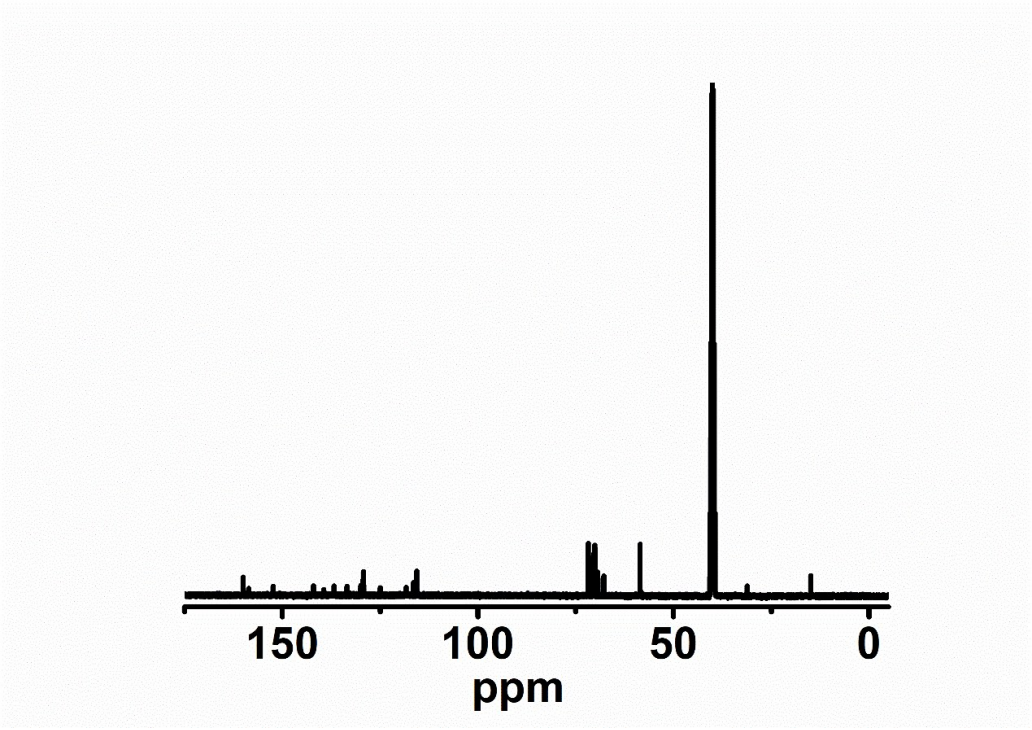

Figure S5. ^{13}C NMR spectrum of MTG-BDP.

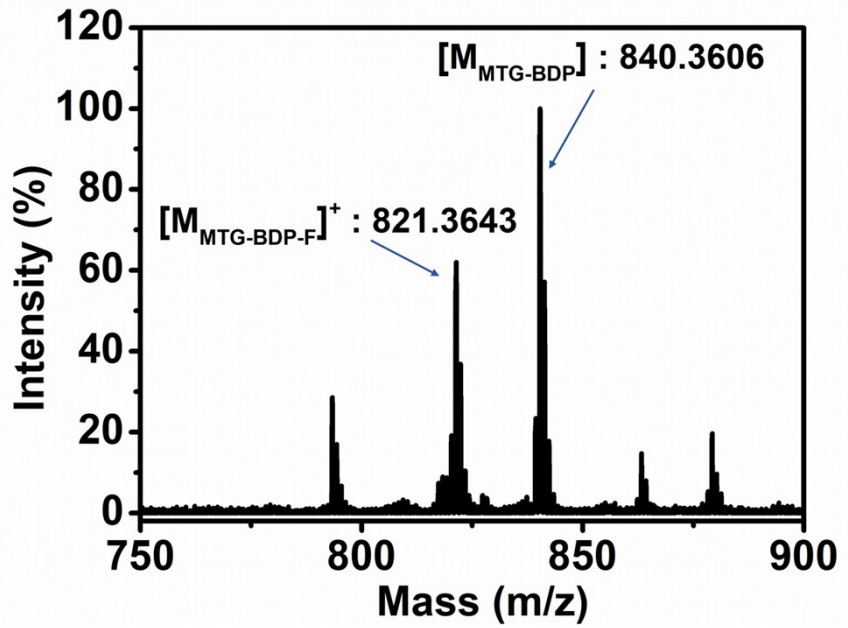

Figure S6. MALDI-TOF of MTG-BDP.

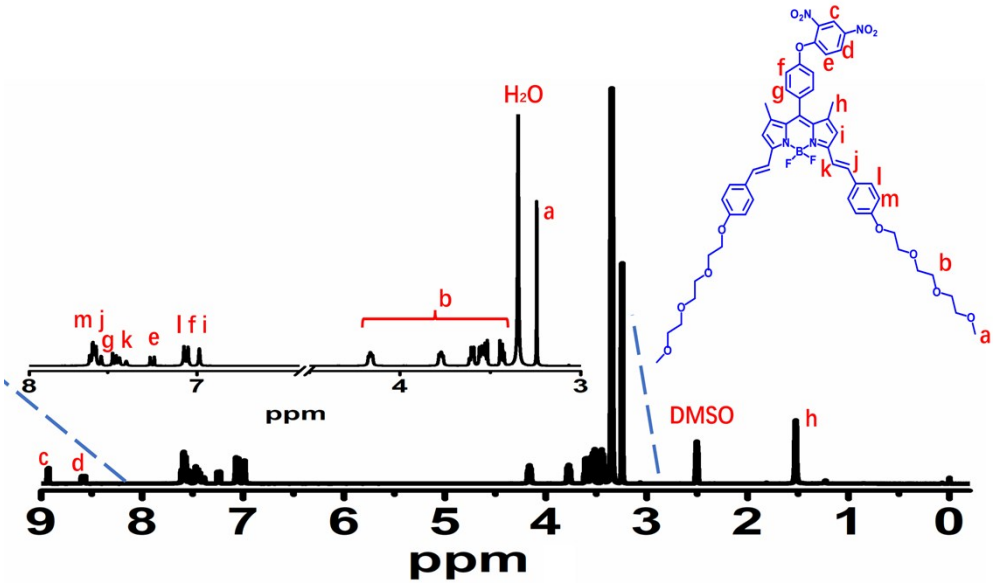

Figure S7. ^{1}H NMR spectrum of DNP-BDP.

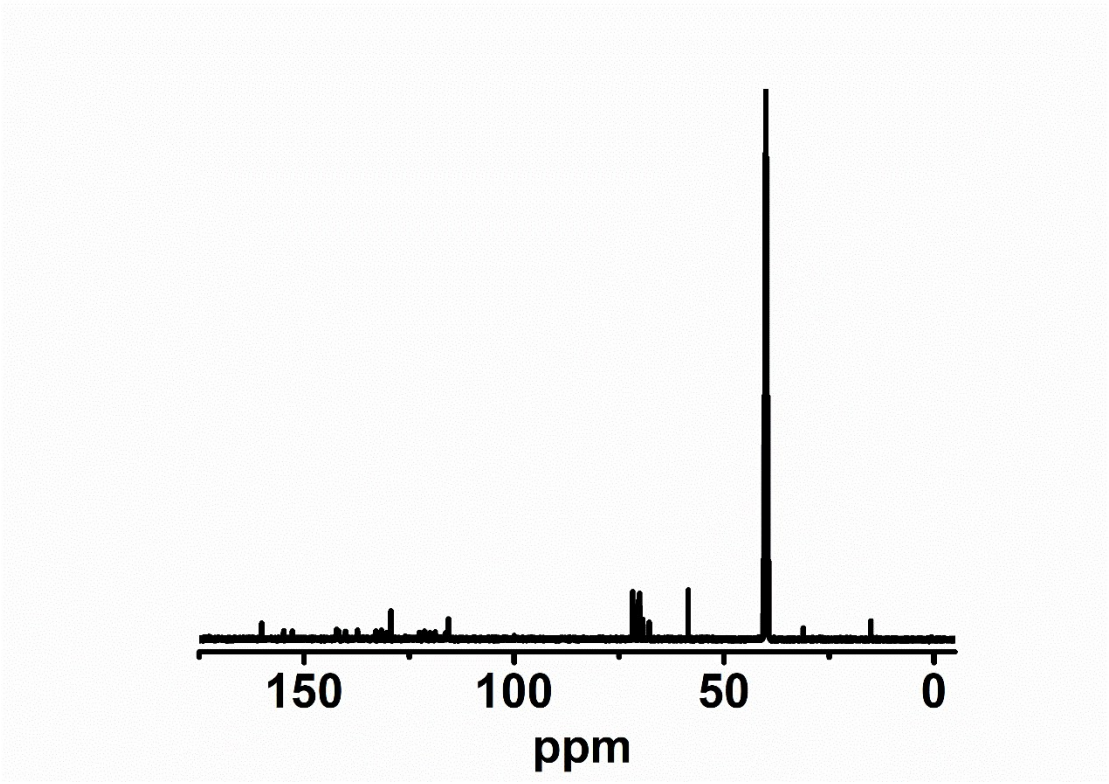

Figure S8. ^{13}C NMR spectrum of DNP-BDP.

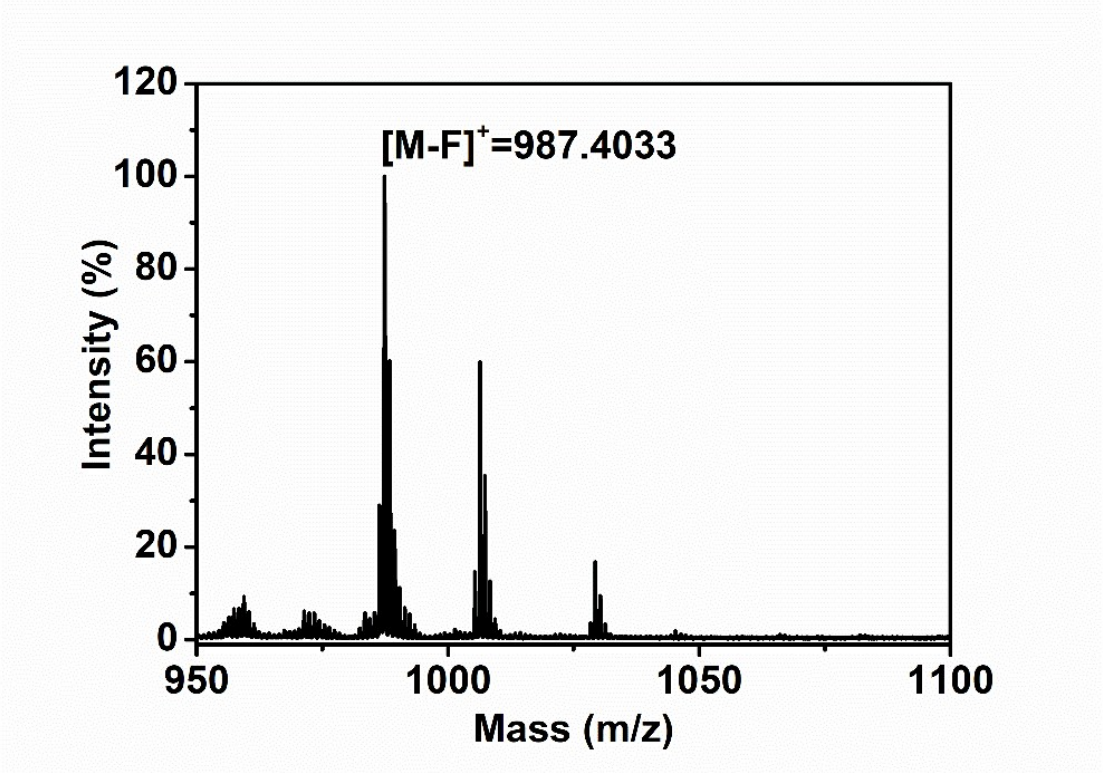

Figure S9. MALDI-TOF of DNP-BDP.

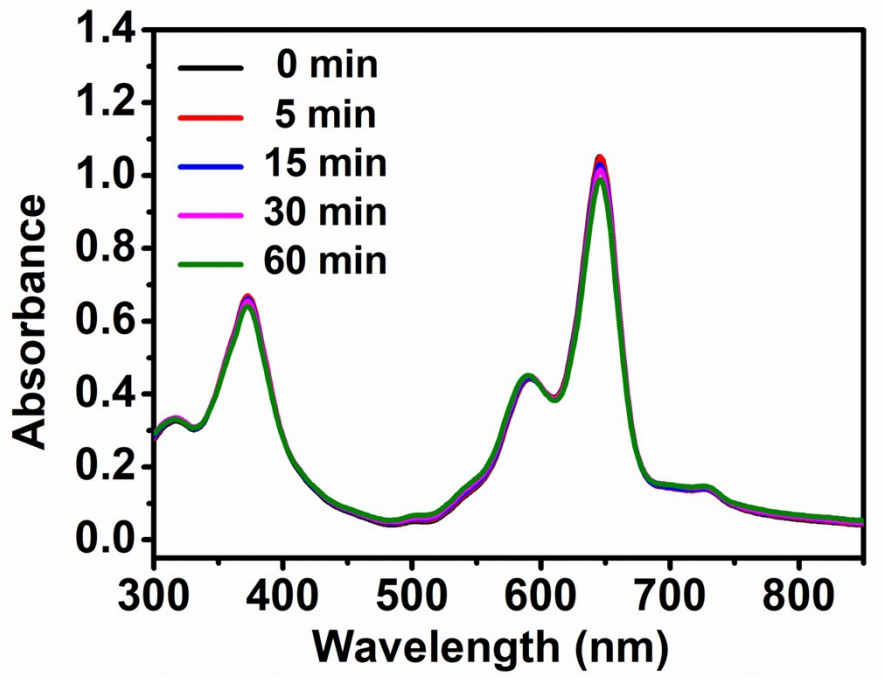

Figure S10. UV-Vis absorption spectra of FR-H_2S in PBS buffer under 650 nm laser irradiation with different time (0.5 W cm^{-2}).

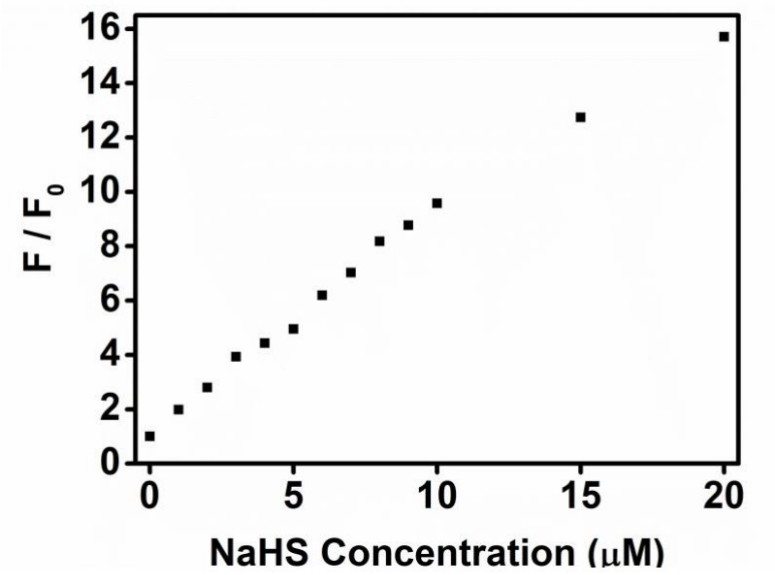

Figure S11. Fluorescence intensity changes of FR-H_2S at 660 nm with the NaHS concentration.

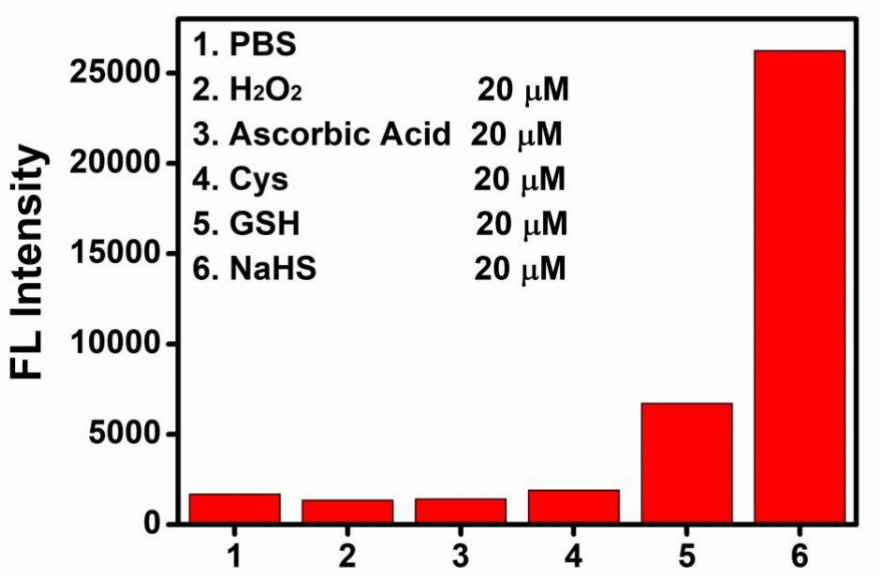

Figure S12. Fluorescence intensity changes of FR-H_2S in the presence of 20 μM NaHS and biologically relevant analytes in PBS (pH 7.4).

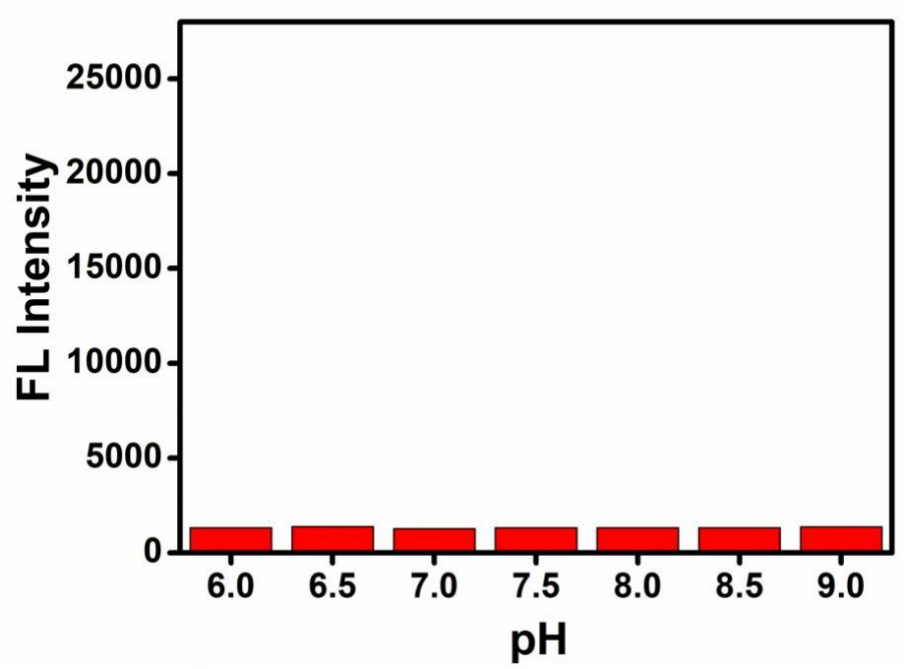

Figure S13. Fluorescence intensity changes of FR-H_2S in different pH.

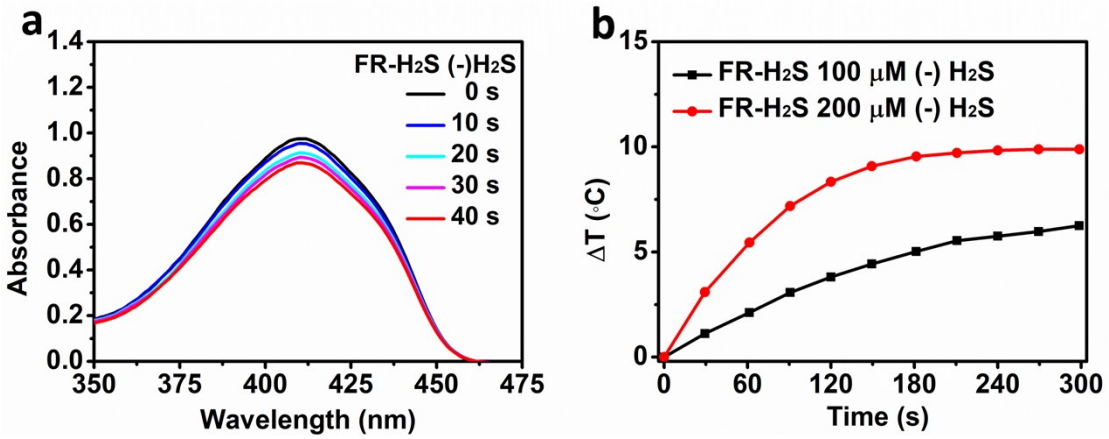

Figure S14. (a) Absorption spectra changes of DPBF upon 650 nm laser irradiation in the presence of FR-H_2S (0.5 W cm^{-2}). (b) Temperature changes for FR-H_2S without NaHS of different concentrations under 650 nm laser irradiation (1 W cm^{-2}).

Table 1. Selected electronic excitation energies (eV) and oscillator strengths (*f*), configurations of the low-lying excited states of DNP-BDP and MTG-BDP calculated by TD//B3LYP/6-31 + G (d, p), based on the optimized ground state geometries. The TDDFT of both molecules in dichloromethane were using the Self Consistent Reaction Field (SCRF) method and the Polarizable Continuum Model (PCM).

BODIPY	Electronic transition	TD//B3LYP/6-31 + G (d, p)			
		Energy/eV [a]	*f* [b]	Composition [c]	CI [d]
DNP-BDP	S0 → S1	1.4903 eV/831.94 nm	0.0002	HOMO → LUMO	0.6716
				HOMO → LUMO + 1	0.2190
	S0 → S2	1.6360 eV/757.83 nm	0.0006	HOMO → LUMO	0.2196
				HOMO → LUMO + 1	0.6716
	S0 → S3	1.9712 eV/628.97 nm	1.1413	HOMO → LUMO + 2	0.7081
MTG-BDP	S0 → S1	1.9818 eV/625.61 nm	1.1564	HOMO → LUMO	0.7080
	S0 → S2	2.7816 eV/445.73 nm	0.3230	HOMO – 1 → LUMO	0.6526
				HOMO → LUMO + 1	0.2666
	S0 → S3	2.9675 eV/417.81 nm	0.0000	HOMO – 2 → LUMO	0.7030

[a]Only the selected low-lying excited states are presented.

[b]Oscillator strength.

[c]Only the main configurations are presented.

[d]The CI coefficients are in absolute values.

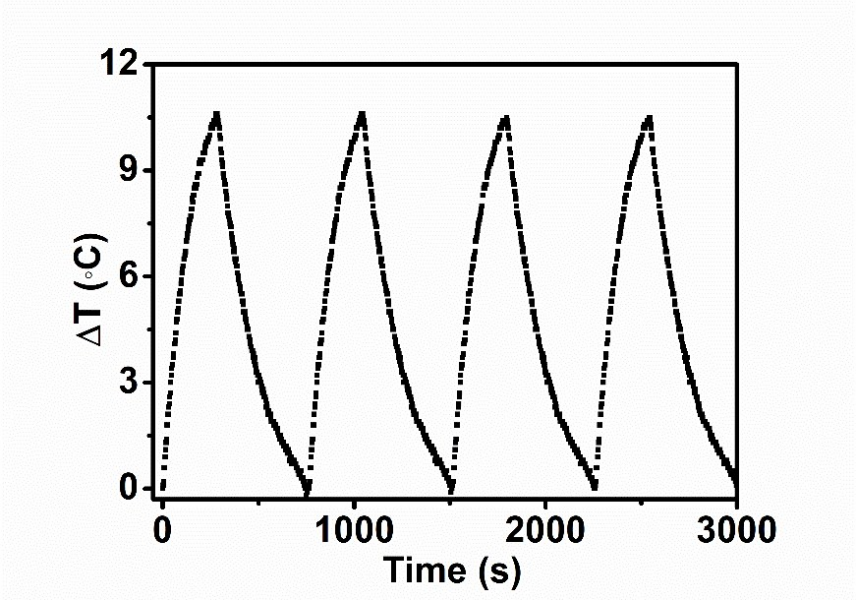

Figure S15. Photothermal stability study of NaHS-pretreated FR-H_2S (50 μM) after 650 nm laser irradiation (0.8 W cm^{-2}).

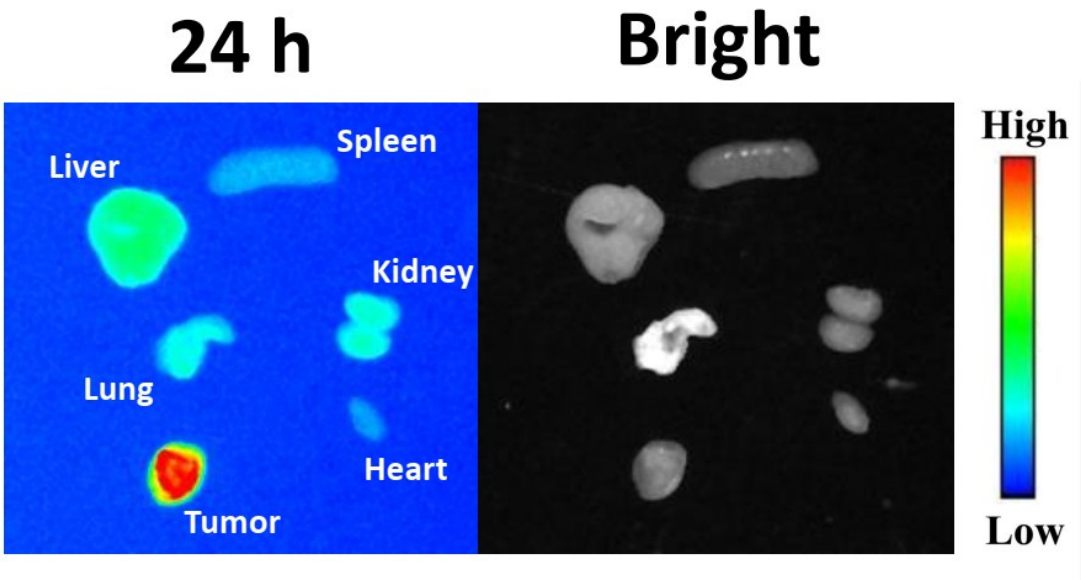

Figure S16. Fluorescence images of organs within 24 h.

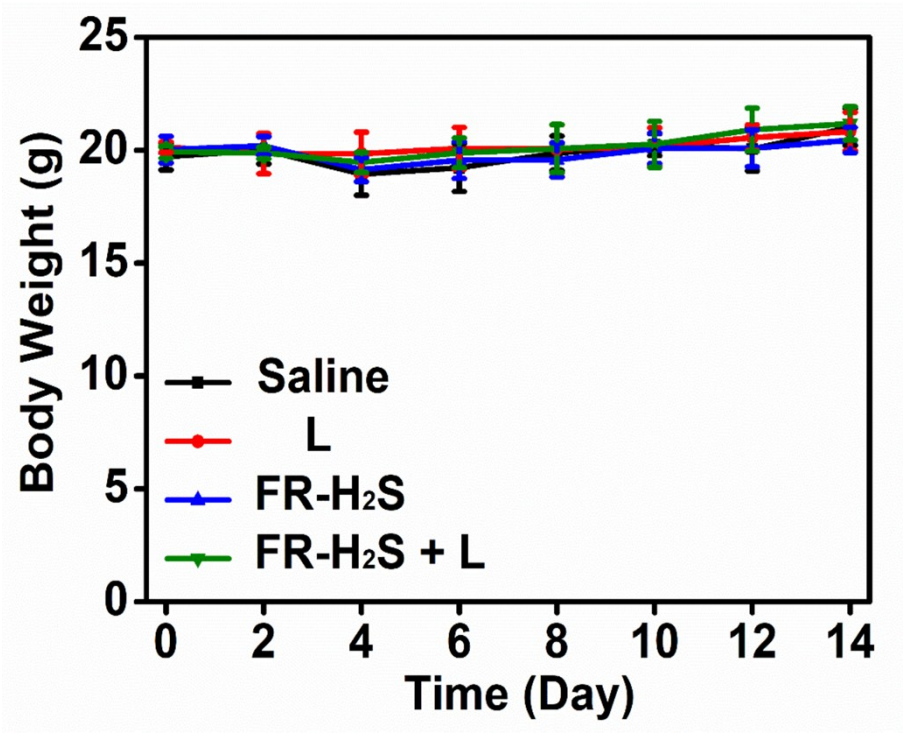

Figure S17. Body weight changes of mice after treatment.

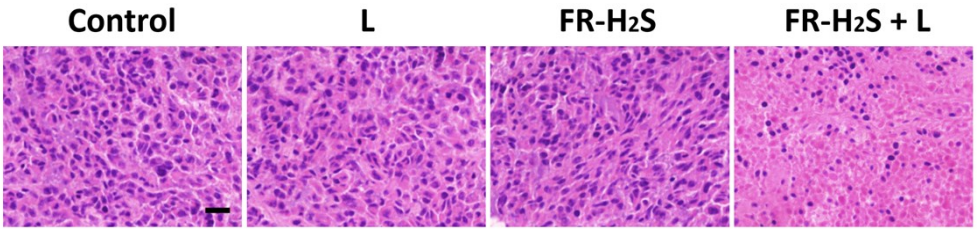

Figure S18. H&E staining of tumors after treatment. Scale bar: 50 μm.

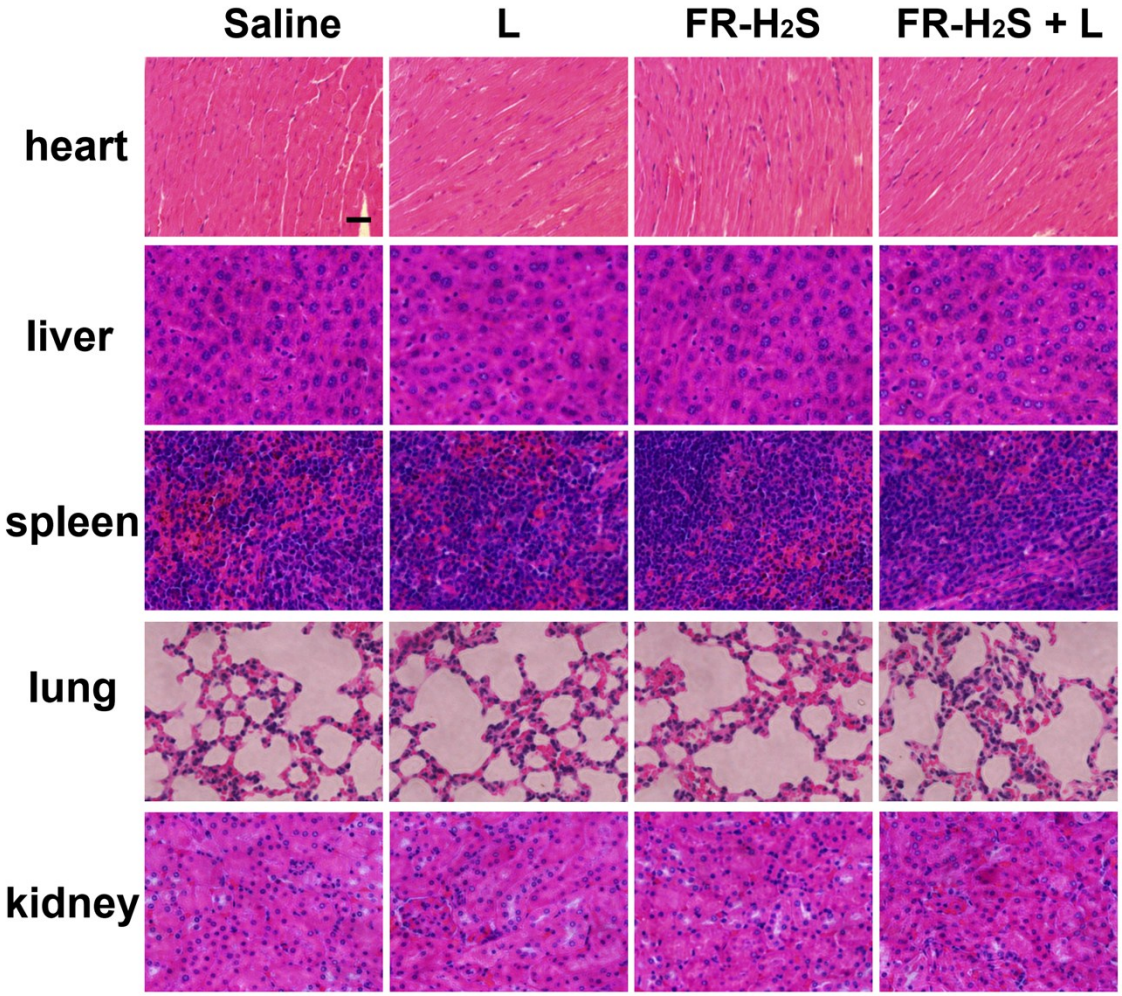

Figure S19. H&E staining of organs after treatment. Scale bar: 50 μm.

Reference

1. S. Roy, D. Samanta, P. Kumar and T. K. Maji, *Chem Commun.* 2018, **54**, 275-278.